Multibody Syst Dyn (2012) 28:157–168
DOI 10.1007/s11044-011-9274-7

Prediction of hip contact forces and muscle activations during walking at different speeds

Luca Modenese · Andrew T.M. Phillips

Received: 19 May 2011 / Accepted: 8 September 2011 / Published online: 5 November 2011
© Springer Science+Business Media B.V. 2011

Abstract The validation of musculoskeletal models is a challenging task necessary to obtain confidence in the numerical predictions they can provide. In this paper, a musculoskeletal model of the lower limb is used to predict the hip contact forces and muscle activations resulting from walking at different speeds for three total hip replacement patients implanted with instrumented prostheses (Bergmann et al., J. Biomech. 34:859–871, 2001). The developed model is shown to estimate the magnitude of hip contact forces with encouraging accuracy in terms of relative peak error (on average within 22% of the experimental value) and global prediction error measurements. Hip contact force predictions were found to be generally more accurate for a slow walking speed. The static optimization technique adopted to estimate muscle activation profiles reproduced for the majority of muscles the modulation and variation in activation patterns documented in the literature for different walking speeds.

Keywords Lower limb · Hip joint contact force · Static optimization · Walking speed · Musculoskeletal model

1 Introduction

The accurate quantification of internal loads acting during human movement has a wide range of applications, from clinical assessment of motor control patterns [1, 2] to prosthesis preclinical testing [3], and as an input for finite element models predicting bone adaptation [4–6]. However, the direct measurement of internal forces developed during human movement is difficult to achieve for practical and ethical reasons. For the lower limb, in vivo joint

Electronic supplementary material The online version of this article (doi:10.1007/s11044-011-9274-7) contains supplementary material, which is available to authorized users.

L. Modenese (✉) · A.T.M. Phillips
Structural Biomechanics, Dept. Civil and Environmental Engineering, Imperial College London, Skempton Building, South Kensington Campus, London, SW7 2AZ, UK
e-mail: l.modenese08@imperial.ac.uk
url: http://www.imperial.ac.uk/structuralbiomechanics

contact forces acting at the hip [7–9] and at the knee [10, 11] have been recorded by instrumented prostheses, but the results are available only for a relatively small set of patients. On the other hand, direct muscle force measurements are generally too invasive to be performed on humans.

Musculoskeletal models of the lower limb have been developed [12, 13] in order to estimate internal loads in the absence of experimental approaches. Usually implemented using specialised multibody software [14–16], these models attempt to estimate the muscle forces necessary to execute a certain task when the kinematics and kinetics are assigned. Static optimization [17] is a technique involving minimisation of a function of the muscle forces, activations or stresses that is often adopted. This framework has been shown to be promising, potentially able to reproduce muscle synergism and advanced muscle recruitment characteristics such as antagonistic muscle co-contractions [18]. Nevertheless, musculoskeletal models are valid only in the measure that they are compared against; this task can be challenging even for simple activities because of the aforementioned lack of experimental measurements. Qualitative validation can be conducted against electromyographic (EMG) signals [19], while some quantitative validations based on joint reaction forces (measured through instrumented prostheses) also exist in the literature [20–22].

This paper introduces a lower limb model based on the Twente Lower Extremity Model (TLEM) dataset [23] and implemented in OpenSim [14]. Previous studies developed musculosketal models after this dataset [24, 25] although only the original authors of the model made an effort toward its validation [24, 26]. To further contribute in this direction the publicly available HIP98 database released by Bergmann and co-workers [7] reporting kinematics, kinetics, and hip contact forces (HCFs) measured on four total hip replacement (THR) patients with instrumented femoral prostheses [27] was used to perform a cycle to cycle validation of the developed model for walking at different speeds. Predicted muscle activations were also checked for consistency against EMG data collected at different walking speeds by previous investigators [28–30].

The aim of this paper is to answer to the following question: is the developed lower limb model able to predict the HCFs and muscle activation variations that have been measured in previous studies through instrumented prostheses and surface electromyography respectively for different walking speeds?

The developed lower limb musculoskeletal model is available for download from http://www.imperial.ac.uk/structuralbiomechanics/3lm.

2 Methods

2.1 The musculoskeletal model

A musculoskeletal model of the lower limb (represented in Fig. 1) was developed in OpenSim [14] based on the TLEM dataset recently collected [23] in order to estimate muscle tensions and HCFs during daily living activities. The unilateral model consists of 6 bodies (pelvis, femur, patella, tibia, hindfoot, and midfoot-phalanxes) connected by 6 joints. The hip joint is represented as a ball and socket joint (3 dofs), the tibio-femoral joint is modeled as a hinge joint (1 dof), and the ankle complex (talocrural and subtalar joints) consists of two hinges (2 dofs). The patella moves along a planar circular path perpendicular to the patello-femoral joint axis (different from the flexion-extension knee axis), dragged by the patellar ligament, which is assumed to be inextensible. Some modifications to the ankle joint axis described in the original dataset were necessary in order to obtain a normal range of motion for the foot. Accounting for the 6 dofs of the pelvis with respect to the ground and

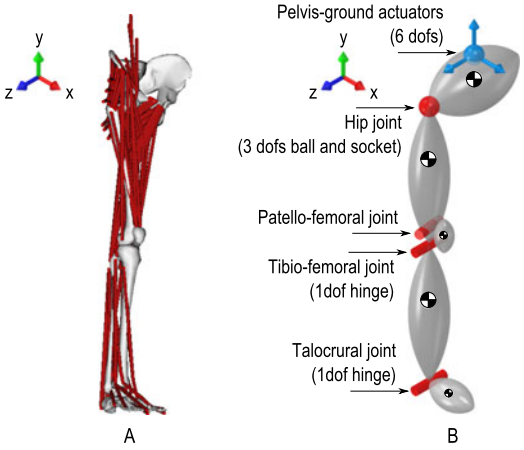

Fig. 1 The musculoskeletal model implemented in OpenSim from the original TLEM dataset (**A**). Six rigid bodies and 163 muscle bundles are included in the model. A multibody representation of the same model (**B**) illustrates the joints and the 11 degrees of freedom of the system used during the simulations

Table 1 General characteristics of the three THR patients taken from [7]

Subject	HIP98 name	Sex	Age	Body weight [N]	Height [m]
S1	HSR	M	55	860	1.74
S2	KWR	M	61	702	1.65
S3	PFL	M	51	980	1.75

considering that during the simulations the subtalar joint was locked, the total number of dofs for the unilateral model is 11. Coordinate systems of the single segments were defined as suggested by the International Society of Biomechanics (ISB) [31].

The lower limb model is comprised of 163 actuators representing 38 muscles, discretised according to a criterion of mechanical equivalence described by van der Helm and Veenbas [32]. Via points and wrapping surfaces were used to enhance the realism of muscle paths influenced by soft tissues and bone structures. A maximal isometric force F_{MAX} proportional to the physiological cross sectional area measured by Horsman and coworkers was defined for each muscle; a muscle tensile stress value of 37 N/cm^2 was chosen [33, 34]. The maximal force was divided equally between individual bundles when a single muscle was represented by multiple actuators. General actuators were included in the model in order to provide the forces and moments necessary to equilibrate the pelvis since the dynamic effects of the torso and the contralateral leg are neglected in the model.

Although muscle contraction dynamics have not been implemented in the model at this stage of development, this has been shown to have a negligible effect on muscle force prediction for walking [35].

2.2 Kinematics and scaling

The kinematics of three patients performing several trials for slow, normal, and fast walking were taken from the HIP98 database. A fourth patient of the database was excluded, as only normal speed walking trials were reported. A general description of the patients and the experimental trials is reported in Tables 1 and 2. Measurements obtained from the same THR patients have been used in previous validation studies [20, 21].

The post-processed markers available in HIP98 were named according to Heller et al. [20] and identified in the general model using the measurements available from the anatom-

Table 2 Average speed and number of trials of each subject for walking at slow, normal and fast velocities, taken from [7]

Subject	Slow walking		Normal walking		Fast walking	
	Trials	Speed [m/s]	Trials	Speed [m/s]	Trials	Speed [m/s]
S1	1	1.04	8	1.36	5	1.64
S2	5	1.05	8	1.15	5	1.40
S3	5	1.02	6	1.13	4	1.40

ical dataset [23]. Manual registration of selected markers was performed for the individualized models. The segment lengths and muscle attachment positions were linearly scaled using the joint centres distances, while femoral geometry (anteversion angle, position of the transition point between prosthesis neck and shaft, angle between the same elements) was implemented based on the HIP98 documentation. The individual masses of the body segments were manually adjusted after the values reported by Bergmann et al. [7], while the adopted inertia tensors were reported by Forster [36] after the values originally published by Heller [37].

The global optimization algorithm described by Lu and O'Connor [38] was finally applied in order to produce the generalized coordinates needed to drive the model. During this operation the maximum tracking error was on average 18.1 mm (17.1 mm for slow walking, 17.5 mm for normal walking, 19.6 mm for fast walking), while the global root mean square error was on average 8.8 mm (8.6 mm for slow walking, 8.6 mm for normal walking, 9.3 mm for fast walking).

2.3 Inverse dynamics analysis

An inverse dynamics analysis was performed using the ground reaction forces and synchronous kinematics reported in HIP98, and the joint intersegmental moments calculated for the model as an open kinetic chain. In particular, the dynamic contribution of the missing torso and contralateral leg to the equilibrium of the pelvis were provided by six general actuators acting on the six pelvis dofs. In OpenSim all the actuators are recruited through minimization of a general objective function (see the following section), but as the ground-pelvis joint is a determinate system the contribution of the general actuators is given by the inverse dynamics results. As a consequence, their weighting on the objective function is a constant in each frame of the kinematics and does not affect the recruitment of the other muscle bundles. These actuators were assigned an F_{MAX} equal to the maximum force calculated by the inverse dynamics in order to guarantee the joint equilibrium throughout all the trials.

2.4 Load sharing problem and muscle forces estimation

Once the intersegmental moments acting on the model joints are known, it is necessary to solve a load sharing problem or distribution problem, i.e. intersegmental loads have to be distributed between the muscles involved in equilibrating the joints [39]. In musculoskeletal models this problem is usually indeterminate, as the muscle actuators crossing a certain joint exceed the number of degrees of freedom of the joint, generating a system that can be equilibrated by different sets of muscle forces. The static optimization technique assumes an optimal strategy underlying the muscle recruitment and can find a unique solution to the load sharing problem.

The optimization problem to be solved for a model having d rotational degrees of freedom and including n muscle actuators is the following:

$$\begin{aligned} &\min \phi(F_i) = \sum_{i=1}^{n} \left(\frac{F_i}{F_{i,\mathrm{MAX}}} \right)^2 \\ &\text{subject to} \quad \sum_{i=1}^{n} \vec{r}_{ij} \times \vec{F}_i = \vec{M}_j, \quad i = 1, \ldots, n, \; j = 1, \ldots, d \\ &\qquad\qquad 0 \leq F_i \leq F_{i,\mathrm{MAX}}, \qquad i = 1, \ldots, n \end{aligned} \tag{1}$$

In the above equation ϕ is the objective function to minimize, F_i the force of the ith muscle, $F_{i,\mathrm{MAX}}$ the maximal force the ith muscle can exert, $\vec{r}_{ij}$ is the moment arm of the ith muscle with respect to the jth rotational dof, and finally $\vec{M}_j$ is the intersegmental moment acting on the jth dof. The ratio between F_i and $F_{i,\mathrm{MAX}}$ is considered as the muscle activation [15, 35], so minimizing the objective function is equivalent to minimizing the sum of squared muscle activations. In this study a nonlinear quadratic objective function [40] has been minimized as it can be demonstrated to produce simultaneous muscle activations consistent with EMG recordings and HCFs comparable with measured values [41].

It is worth noticing that this technique can be used to solve the load sharing problem for fully dynamic tasks and the adjective 'static' in the name is due to the fact that the motion is solved frame by frame independently, as in a static problem.

2.5 Hip contact forces

HCFs were calculated from the muscle forces obtained through static optimization. A detailed comparison of the model predictions with respect to the HCFs measured by Bergmann et al. [7] is provided both in terms of peak and global estimation error. At the frame of experimental peak (where kinematics and kinetics lead to the maximum measured HCFs) the following parameters have been calculated to assess the model predictions:

(1) The relative error for the resultant force (as a percentage of the experimental peak). To avoid cancellations due to opposite signs, the absolute values obtained from the trials were averaged.
(2) The predicted and measured HCFs components expressed in the ISB recommended femoral reference system [31] were compared. In brief, for the left leg in the reference position the X axis points anteriorly, the Y axis cranially and the Z axis medially [31].

The model predictions over the entire gait cycle were then assessed by calculating the following indicators:

(1) The average trial deviation, calculated as the average difference between experimental and numerical HCFs through each trial frame. A mean value and a range are provided from all the trials of each subject.
(2) The Pearson's correlation coefficient (R) to quantify the similarity in shape of the predicted and measured force resultants.
(3) The root mean squared error (RMSE), as a global indicator of the fit goodness.

2.6 Muscle forces

Activations of specific muscles that have been observed to be influenced by gait speed [28–30, 42] are reported, in order to assess if the model can predict these changes. *Tibialis*

anterior, *gastrocnemius medialis*, *soleus*, *rectus femoris*, medial hamstring, *vastus lateralis*, and *gluteus medius* are considered.

Since in the developed model some muscles are modelled by several bundles, a mean activation has been calculated. Subject S1 has been chosen as representative for discussion purposes, presenting the largest speed difference between slow and fast walking.

3 Results

In Fig. 2, a visual comparison between the magnitudes of the measured and predicted HCFs is presented for slow, normal, and fast walking.

The values of the average errors at the experimental peak frame are reported in Table 3. The general tendency of the model is to underestimate the experimental peak for slow walking and overestimate it for normal and fast walking. The relative error is in a range from 0.2% to 22% of the experimental peak value. Individual HCF components expressed in the femoral coordinate system are compared in Fig. 3; in the anterior-posterior (X axis) and medio-lateral (Z axis) directions, respectively, the model under and overestimates the absolute measured force, so giving a resultant oriented less posteriorly and more laterally than the experimental. This is particularly evident for the Z direction.

The RSME averaged for the activity trials is presented for each subject in Fig. 4, which suggests that the global goodness of fit is generally decreasing as walking speed increases (S2 is an exception having lower RMSE for normal than slow walking). The range of values of R (Table 3) calculated for the individual trials indicate a strong correlation between mea-

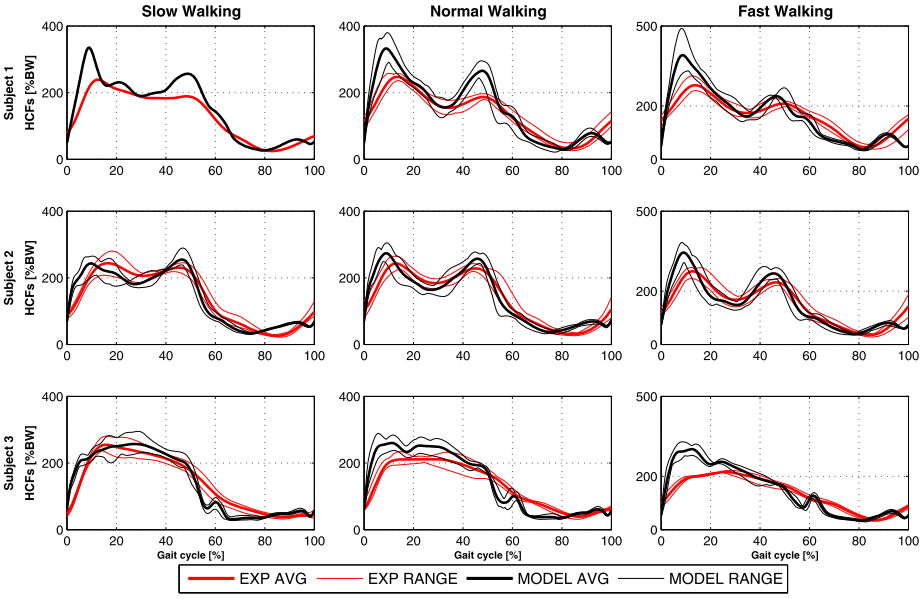

Fig. 2 (Color online) Hip contact force magnitudes measured in vivo (in *red*), taken from [7] and those predicted by the model (in *black*) for three subjects walking at three different speeds. The average magnitude is represented as a *thick line*, the range boundaries as *thin lines*

Table 3 Average error at the frame of experimental peak, average trial deviation mean and range (minus indicates underestimation) and the Pearson's correlation coefficient R, reported for each walking speed

Activity	Subject	Relative error at exp peak [% Exp peak]	Average trial deviation mean [% BW]	Average trial deviation range [% BW]	R^c [range]
Slow walking	S1[a]	16.2	21.7	–	0.95
	S2	10.9[b]	−1.4	−8.9–8.5	0.88–0.96
	S3	4.1[b]	−0.1	−3.6–3.1	0.93–0.96
Normal walking	S1	16.3	17.3	9.5–25.5	0.91–0.94
	S2	0.2[b]	1.8	−2.3–8.2	0.90–0.96
	S3	10.4	9.8	4.6–20.4	0.91–0.94
Fast walking	S1	22.0	5.0	−3.5–18.5	0.86–0.93
	S2	7.9	2.4	−0.3–8.2	0.88–0.95
	S3	14.9	12.0	8.0–15.0	0.88–0.90

[a]Only one trial of slow walking was available for S1

[b]If the arithmetic average is considered the value would be negative, indicating underestimation at the experimental peak

[c] $p < 0.01$ for all R

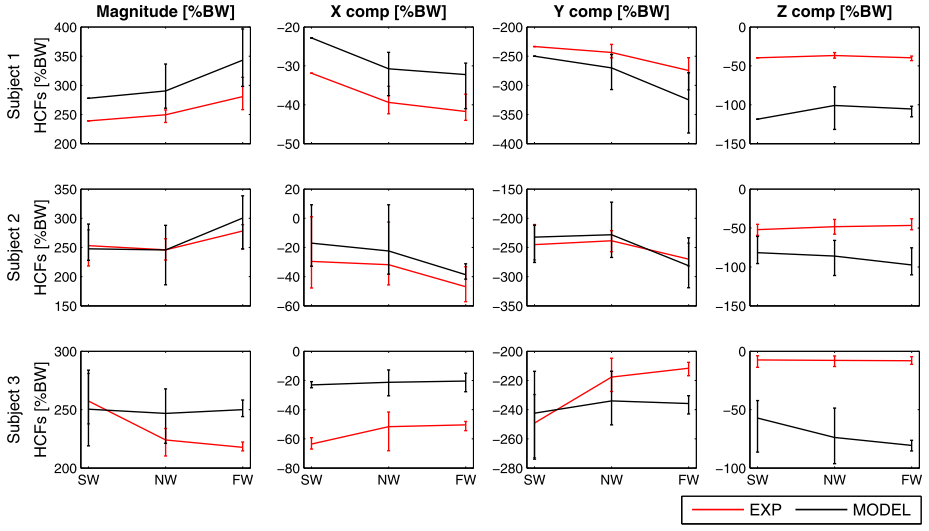

Fig. 3 (Color online) Average magnitudes and component values of the measured (in *red*), taken from [7] and numerical (in *black*) hip contact forces (HCFs) compared at the frame of experimental peak for three subjects walking at three different speeds. The force components are expressed in the ISB femoral local reference system [28]. The error bars represent the range

sured and predicted HCFs. Average trial deviation mean and range are reported in Table 3. The average trial deviation mean is smaller than 22% BW (18% if the single trial of slow walking for Subject S1 is excluded) for all subjects.

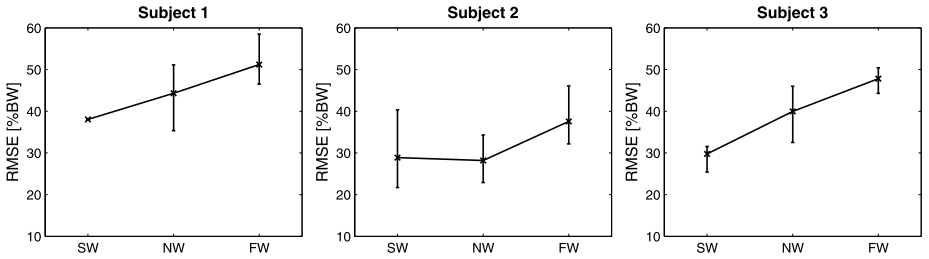

Fig. 4 Average root mean square error calculated for each subject for slow walking (SW), normal walking (NW) and fast walking (FW). The error bars represent the range

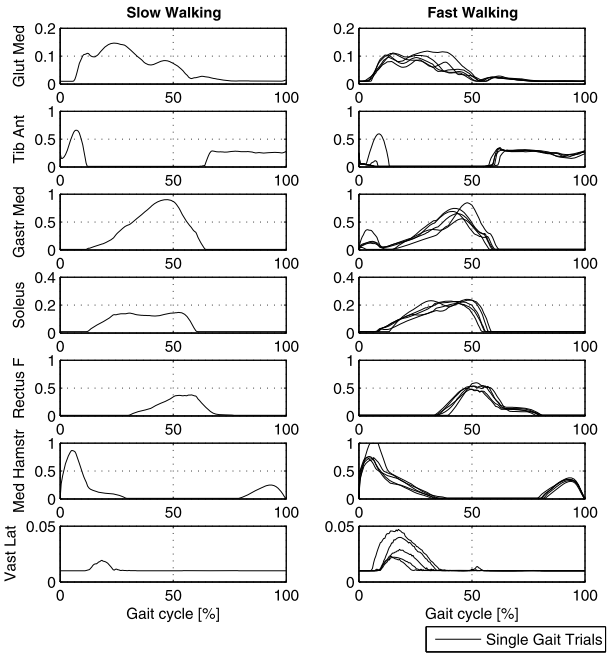

Fig. 5 Muscle activations estimated for Subject S1 during slow and fast walking. The activation of each muscle is represented by a single line for each trial and all simulated trials are plotted. Average toe off is around 60% of the gait cycle. The following muscles are represented: *gluteus medius*, *tibialis anterior*, *gastrocnemius medialis*, *soleus*, *rectus femoris*, medial hamstrings (summation of *semimembranosus* and *semitendinosus*), and *vastus lateralis*

Muscle activations obtained for slow and fast walking are compared for Subject S1 in Fig. 5. The same comparison for the other subjects is available in the electronic supplementary material.

4 Discussion

In this paper the gait of three THR [7] patients was simulated using a musculoskeletal model of the lower limb, in order to accurately assess its predictive potential for HCFs and muscle activities over a range of walking speeds.

The HCFs calculated by the model have been shown to predict with an encouraging degree of accuracy the experimental peak: relative estimation errors did not exceed 10.9% when underestimating the peak and 22.0% when overestimating it. These results are in line with previous validations [20, 21], which adopted linear muscle recruitment criteria, gener-

ally unable to reproduce muscle synergism [43]. The HCFs component analysis reported in Fig. 3 shows magnitude underestimation of the reaction force in the anterior-posterior direction and magnitude overestimation in the medio-lateral direction for all the walking speeds. This may happen for two reasons:

(1) A straight line between the origin and insertion of *gluteus maximus* and *gluteus medius* may lead to underestimation of the moment arm with respect to the hip joint centre, causing higher muscle activation as a consequence of the higher force needed to equilibrate the intersegmental moments.
(2) Postoperative abductor muscles weakness in THR patients [44, 45] (possibly due to denervation [46, 47]) was not represented in the lower limb model. This condition could alter the muscle recruitment requiring less activation from the abductor muscles.

RMSE and R values suggest that the HCFs are better predicted throughout the gait cycle for slow walking speeds. The reason for this could be that the influence of muscle dynamics on muscle force estimation is not negligible for all walking speeds (the study of Anderson and Pandy [35] refers to a speed of 1.35 m/s).

With increasing walking speed, experimentally recorded EMG patterns exhibit amplitude modulation and for some muscles modification of the phases of activity [28, 29, 42, 48]. For instance, the *gastrocnemius* EMG activity normally presents a single peak in late stance, while for high walking speeds a second peak during early stance has been observed [28]. This feature has been predicted by the model, as can be seen in Fig. 5. Also, the behaviour of *rectus femoris* described in the investigation of Nene et al. [30] was recognisable in our simulations and generally the numerical results for this muscle were consistent with the fine wire EMG data reported in that study and with the EMG profiles published by Perry [49] for normal walking. Both a biphasic [50] and monophasic [29, 30] activation has been reported for *vastus lateralis* during slow speed gait, and a certain variability in the activation pattern has also been observed in normal walking [50, 51]. However, the EMG profile becomes monophasic as speed increases, with a single peak in early stance [28–30]. Although a minor muscle activation was predicted, simulation results produced a single peak during stance for slow walking, and a small second peak around toe off during fast walking. Finally, modulation of muscle activation is recognizable in most muscles plotted in Fig. 5 except *tibialis anterior* and *gluteus medius* that seem not to modify their level. Consistent EMG activation across different walking speeds was recorded for the *tibialis anterior* by previous investigators [28, 29], while the *gluteus medius* load insensitive behaviour may be due to the intersection of some of its bundles with *gluteus maximus* bundles. In conjunction with the medial hip contact force component overestimation, an improvement in the modelling of the muscle layers of the hip seems mandatory to improve HCFs predictions.

As a final remark, it is noted that the trials here considered as fast walking (on average 1.64 m/s for S1), although consistent with other postoperative gait measurements in THR patients [52], are actually quite slow if compared to fast walking speed in the referenced EMG literature, e.g. 1.92 m/s [42] and 1.81 m/s [28]. This could have affected the comparison with EMG studies by making changes in muscle activation less evident.

5 Summary

A musculoskeletal model of the lower limb was developed to simulate walking at different speeds and predict muscle activation patterns and hip contact forces. The comparison of the estimated internal forces against measurements obtained by instrumented prostheses

[7] and EMG recordings available in the literature suggest that the model can predict with satisfactory accuracy both the magnitude of HCFs and the muscle activation patterns with varying walking speeds.

The results of this study are particularly encouraging because they represent a validation of the musculoskeletal model over the same task executed with different modalities. Results indicate a need to enhance the geometrical modelling of the gluteal muscles. A more accurate representation of muscle layers seems necessary to improve estimation of both HCFs and muscle activation patterns. More generally, muscle dynamics should be implemented in the model in order to investigate high speed activities.

References

1. Jonkers, I., Stewart, C., Spaepen, A.: The study of muscle action during single support and swing phase of gait: clinical relevance of forward simulation techniques. Gait Posture **17**(2), 97–105 (2003)
2. Steele, K.M., Seth, A., Hicks, J.L., Schwartz, M.S., Delp, S.L.: Muscle contributions to support and progression during single-limb stance in crouch gait. J. Biomech. **43**(11), 2099–2105 (2010)
3. Heller, M.O., Bergmann, G., Kassi, J.P., Claes, L., Haas, N.P., Duda, G.N.: Determination of muscle loading at the hip joint for use in pre-clinical testing. J. Biomech. **38**(5), 1155–1163 (2005)
4. Bitsakos, C., Kerner, J., Fisher, I., Amis, A.A.: The effect of muscle loading on the simulation of bone remodelling in the proximal femur. J. Biomech. **38**(1), 133–139 (2005)
5. Geraldes, D.M., Phillips, A.T.M.: 3D strain-adaptive continuum orthotropic bone remodelling algorithm: prediction of bone architecture in the femur. In: Lim, C.T., Goh, J.C.H. (eds.) 6th World Congress of Biomechanics (WCB 2010), 1–6 August 2010, Singapore, vol. 31, pp. 772–775. Springer, Berlin (2010)
6. Phillips, A.T.M.: Structural optimisation: biomechanics of the femur. In: Proceedings of the ICE. Engineering and Computational Mechanics, vol. 165 (2012, in press)
7. Bergmann, G., Deuretzbacher, G., Heller, M., Graichen, F., Rohlmann, A., Strauss, J., Duda, G.N.: Hip contact forces and gait patterns from routine activities. J. Biomech. **34**(7), 859–871 (2001)
8. Rydell, N.W.: Forces acting on the femoral head-prosthesis. A study on strain gauge supplied prostheses in living persons. Acta Orthop. Scand. **37**(Supplement 88), 81–132 (1966)
9. Davy, D.T., Kotzar, G.M., Brown, R.H., Heiple, K.G., Goldberg, V.M., Heiple, K.G., Jr., Berilla, J., Burstein, A.H.: Telemetric force measurements across the hip after total arthroplasty. J. Bone Jt. Surg. (Am. Ed.) **70**(1), 45–50 (1988)
10. D'Lima, D.D., Patil, S., Steklov, N., Chien, S., Colwell, C.W., Jr.: In vivo knee moments and shear after total knee arthroplasty. J. Biomech. **40**(Supplement 1), S11–S17 (2007)
11. Kutzner, I., Heinlein, B., Graichen, F., Bender, A., Rohlmann, A., Halder, A., Beier, A., Bergmann, G.: Loading of the knee joint during activities of daily living measured in vivo in five subjects. J. Biomech. **43**(11), 2164–2173 (2010)
12. Delp, S.L., Loan, J.P., Hoy, M.G., Zajac, F.E., Topp, E.L., Rosen, J.M.: An interactive graphics-based model of the lower extremity to study orthopaedic surgical procedures. IEEE Trans. Biomed. Eng. **37**(8), 757–767 (1990)
13. Brand, R.A., Crowninshield, R.D., Wittstock, C.E., Pedersen, D.R., Clark, C.R., van Krieken, F.M.: A model of lower extremity muscular anatomy. J. Biomech. Eng. **104**(4), 304–310 (1982)
14. Delp, S.L., Anderson, F.C., Arnold, A.S., Loan, P., Habib, A., John, C.T., Guendelman, E., Thelen, D.G.: OpenSim: open-source software to create and analyze dynamic simulations of movement. IEEE Trans. Biomed. Eng. **54**(11), 1940–1950 (2007)
15. Damsgaard, M., Rasmussen, J., Christensen, S.T., Surma, E., de Zee, M.: Analysis of musculoskeletal systems in the AnyBody Modeling System. Simul. Model. Pract. Theory **14**(8), 1100–1111 (2006)
16. Sherman, M.A., Seth, A., Delp, S.L.: Simbody: multibody dynamics for biomedical research. Procedia IUTAM **2**, 241–261 (2011)
17. Tsirakos, D., Baltzopoulos, V., Bartlett, R.: Inverse optimization: functional and physiological considerations related to the force-sharing problem. Crit. Rev. Biomed. Eng. **25**(4–5), 371–407 (1997)
18. Jinha, A., Ait-Haddou, R., Binding, P., Herzog, W.: Antagonistic activity of one-joint muscles in three-dimensions using non-linear optimisation. Math. Biosci. **202**(1), 57–70 (2006)
19. Erdemir, A., McLean, S., Herzog, W., van den Bogert, A.J.: Model-based estimation of muscle forces exerted during movements. Clin. Biomech. **22**(2), 131–154 (2007)
20. Heller, M.O., Bergmann, G., Deuretzbacher, G., Dürselen, L., Pohl, M., Claes, L., Haas, N.P., Duda, G.N.: Musculo-skeletal loading conditions at the hip during walking and stair climbing. J. Biomech. **34**(7), 883–893 (2001)

21. Stansfield, B.W., Nicol, A.C., Paul, J.P., Kelly, I.G., Graichen, F., Bergmann, G.: Direct comparison of calculated hip joint contact forces with those measured using instrumented implants. An evaluation of a three-dimensional mathematical model of the lower limb. J. Biomech. **36**(7), 929–936 (2003)
22. Nikooyan, A.A., Zadpoor, A.A.: An improved cost function for modeling of muscle activity during running. J. Biomech. **44**(5), 984–987 (2011)
23. Klein Horsman, M.D., Koopman, H.F., van der Helm, F.C., Prose, L.P., Veeger, H.E.: Morphological muscle and joint parameters for musculoskeletal modelling of the lower extremity. Clin. Biomech. **22**(2), 239–247 (2007)
24. Klein Horsman, M.D.: The Twente lower extremity model. Ph.D. thesis, University of Twente (2007)
25. Cleather, D.J., Bull, A.M.J.: Lower-extremity musculoskeletal geometry affects the calculation of patellofemoral forces in vertical jumping and weightlifting. Proc. Inst. Mech. Eng., H J. Eng. Med. **224**(9), 1073–1083 (2010)
26. Koopman, H.F.J.M., Klein Horsman, M.D.: Hip compression force estimation with a comprehensive musculoskeletal model. In: Spink, A.J., Ballintijn, M.R., Bogers, N.D., Grieco, F., Loijens, L.W.S., Noldus, L.P.J.J., Smit, G., Zimmermann, P.H. (eds.) Proceeding of Measuring Behavior 2008, 6th Conference on Methods and Techniques in Behavioural Research, Maastricht, The Netherlands, p. 16 (2008)
27. Graichen, F., Bergmann, G., Rohlmann, A.: Hip endoprosthesis for in vivo measurement of joint force and temperature. J. Biomech. **32**(10), 1113–1117 (1999)
28. Shiavi, R., Bugle, H.J., Limbird, T.: Electromyographic gait assessment, Part 1: Adult EMG profiles and walking speed. J. Rehabil. Res. Dev. **24**(2), 13–23 (1987)
29. Yang, J.F., Winter, D.A.: Surface EMG profiles during different walking cadences in humans. Electroencephalogr. Clin. Neurophysiol. **60**(6), 485–491 (1985)
30. Nene, A., Byrne, C., Hermens, H.: Is rectus femoris really a part of quadriceps? Assessment of rectus femoris function during gait in able-bodied adults. Gait Posture **20**(1), 1–13 (2004)
31. Wu, G., Siegler, S., Allard, P., Kirtley, C., Leardini, A., Rosenbaum, D., Whittle, M., D'Lima, D.D., Cristofolini, L., Witte, H., Schmid, O., Stokes, I.: ISB recommendation on definitions of joint coordinate system of various joints for the reporting of human joint motion—part I: ankle, hip, and spine. J. Biomech. **35**(4), 543–548 (2002)
32. Van der Helm, F.C., Veenbaas, R.: Modelling the mechanical effect of muscles with large attachment sites: application to the shoulder mechanism. J. Biomech. **24**(12), 1151–1163 (1991)
33. Weijs, W.A., Hillen, B.: Cross-sectional areas and estimated intrinsic strength of the human jaw muscles. Acta Morphol. Neerl.-Scand. **23**(3), 267–274 (1985)
34. Haxton, H.A.: Absolute muscle force in the ankle flexors of man. J. Physiol. **103**(3), 267–273 (1944)
35. Anderson, F.C., Pandy, M.G.: Static and dynamic optimization solutions for gait are practically equivalent. J. Biomech. **34**(2), 153–161 (2001)
36. Forster, E.: Predicting muscle forces in the human lower limb during locomotion. University of Ulm (2003)
37. Heller, M.: Muskuloskelettale Belastungen nach Totalhüftarthroplastick. University of Ulm (2002)
38. Lu, T.W., O'Connor, J.J.: Bone position estimation from skin marker co-ordinates using global optimisation with joint constraints. J. Biomech. **32**(2), 129–134 (1999)
39. Crowninshield, R.D., Brand, R.A.: The prediction of forces in joint structures: distribution of intersegmental resultants. Exerc. Sport Sci. Rev. **9**(1), 159–182 (1981)
40. Pedotti, A., Krishnan, V.V., Stark, L.: Optimization of muscle-force sequencing in human locomotion. Math. Biosci. **38**, 57–76 (1978)
41. Modenese, L., Phillips, A.T.M., Bull, A.M.J.: An open source lower limb model: Hip joint validation. J. Biomech. **44**(12), 2185–2193 (2011)
42. Murray, M.P., Mollinger, L.A., Gardner, G.M., Sepic, S.B.: Kinematic and EMG patterns during slow, free, and fast walking. J. Orthop. Res. **2**(3), 272–280 (1984)
43. Pedersen, D.R., Brand, R.A., Cheng, C., Arora, J.S.: Direct comparison of muscle force predictions using linear and nonlinear programming. J. Biomech. Eng. **109**, 192–200 (1987)
44. Long, W.T., Dorr, L.D., Healy, B., Perry, J.: Functional recovery of noncemented total hip arthroplasty. Clin. Orthop. Relat. Res. **288**, 73–77 (1993)
45. Murray, M.P., Gore, D.R., Brewer, B.J., Mollinger, L.A., Sepic, S.B.: Joint function after total hip arthroplasty: a four-year follow-up of 72 cases with Charnley and Müller replacements. Clin. Orthop. Relat. Res. **157**, 119–124 (1981)
46. Baker, A., Bitounis, V.: Abductor function after total hip replacement. An electromyographic and clinical review. J. Bone Jt. Surg., Br. Vol. **71-B**(1), 47–50 (1989)
47. Kenny, P., O'Brien, C.P., Synnott, K., Walsh, M.G.: Damage to the superior gluteal nerve after two different approaches to the hip. J. Bone Jt. Surg., Br. Vol. **81-B**(6), 979–981 (1999)
48. Nilsson, J., Thorstensson, A.L.F., Halbertsma, J.: Changes in leg movements and muscle activity with speed of locomotion and mode of progression in humans. Acta Physiol. Scand. **123**(4), 457–475 (1985)

49. Perry, J.: Hip. In: Gait analysis: normal and pathologic function, pp. 111–129. SLACK Incorporated, Thorofare (1992)
50. Wootten, M., Kadaba, M., Cochran, G.: Dynamic electromyography. II. Normal patterns during gait. J. Orthop. Res. **8**(2), 259–265 (1990)
51. Winter, D.A., Yack, H.J.: EMG profiles during normal human walking: stride-to-stride and inter-subject variability. Electroencephalogr. Clin. Neurophysiol. **67**(5), 402–411 (1987)
52. Shih, C.-H., Du, Y.-K., Lin, Y.-H., Wu, C.-C.: Muscular recovery around the hip joint after total hip arthroplasty. Clin. Orthop. Relat. Res. **302**, 115–120 (1994)